Solubility of Gold in Common Gold-Concentrating Minerals

V.L. Tauson✉, S.V. Lipko

A.P. Vinogradov Institute of Geochemistry, Siberian Branch of the Russian Academy of Sciences, ul. Favorskogo 1a, Irkutsk, 664033, Russia

Abstract—The paper is a summary of the authors' and published data on the occurrence of Au in common gold-concentrating minerals (pyrite, arsenopyrite, pyrrhotite, chalcopyrite, bornite, galena, sphalerite, and magnetite). The solubility of gold in minerals is evaluated through identification of the limiting element incorporation into the real crystal. The distribution of gold between coexisting minerals is considered. Obtaining reliable data on the gold solubility involves discrimination of the structural form of the element and correct separation of Au forms between the surface and the volume, which is not always possible because of the small size and low quality of crystals (defects and highly developed internal surfaces). It is also necessary to have a phase (individual or nonautonomous) limiting the incorporation of Au or to compare the mineral under study (within the framework of the principle of phase composition correlation) with a reference mineral with a reliably established structural form of Au. The most reliable and consistent estimates for the hydrothermal parameters (450–500 ºC, 1 kbar) are as follows (µg/g): sphalerite – 0.7, highly ferrous sphalerite – 5, magnetite – 1, pyrite – 3, manganese and copper-containing pyrite – 10, pyrrhotite – 21, chalcopyrite – 110, bornite – 140, and galena – 240. The highest solubility of gold (up to 30,000 µg/g) is established in arsenopyrite, but it is likely to be a metastable miscibility caused by the nonstationary conditions of crystal growth or by the crystal growth at the expense of the surficial nonautonomous phase. The same factors can cause supersaturation of pyrite with Au admixture at low temperatures. The dual behavior of Au in pyrrhotite and magnetite is for a different reason: Under reducing conditions, these minerals can contain a submicroscopic elemental form of Au indistinguishable from the structural one. We consider the forms of Au occurrence and the relationship between the solubility of gold and its metallic bonds in minerals.

Keywords: gold; solubility; pyrite; arsenopyrite; pyrrhotite; chalcopyrite; bornite; galena; sphalerite; magnetite

INTRODUCTION

More than 30 years have passed since the publication of the first works on methods and results for determining the solubility and distribution of gold in sulfide minerals (Mironov and Geletii, 1979; Mironov et al., 1987, 1989). The attempts to understand the problem following the above studies were of fragmentary character. Generalization and analysis of results, with rare exceptions (Tauson et al., 1996; Tauson and Lipko, 2015), were absent, despite the power of new analytical methods. It appears that, as was in many respects explained by the observation of S.P. Kapitsa (1991): "If the computer is unsurpassed in its ability to process numbers and information, then until we determine the initial concepts and learn to measure them, all the power of artificial intelligence will not be able to help the infirmity of our natural consciousness". This is especially true for the geological sciences, where universal laws and their numerical characteristics are still insufficiently used. The purpose of this paper is to consider the regularities and factors of gold occurrence in the structures of ore minerals on the basis of modern concepts, methods and methodological approaches.

The significance of the structurally bound form of Au is without doubt, since it provides an opportunity to make comparative estimates of the metal content in ore-forming fluids that form gold deposits, based on experimental data on the mineral-hydrothermal solution distribution coefficient (Tauson et al., 2018b). It is the only indicator of the element activity in a hydrothermal solution. At present, there is an urgent need to gather together the data we previously obtained on the incorporation of Au into its main concentrator minerals and compare them with the existing estimates and global data obtained by the state-of-the-art methods. This will allow us to objectively assess the state of the problem and the most important theoretical and practical trends for further research. This work is based largely on experimental data. Natural data on Au content in minerals are unlikely to be instrumental in solving the problem of the limits of gold incorporation in them due to very rough ideas about conditions and mechanisms of their formation and post-growth history.

CONCEPTS AND DEFINITIONS, METHODOLOGY

This paper uses a system of concepts proposed by one of the authors (Tauson, 1999a, 2005) based on solid state geo-

✉Corresponding author.
   E-mail address: vladimir_tauson@mail.ru (V.L. Tauson)

chemistry concepts (Urusov et al., 1997). Many authors believe that the solubility of Au in a mineral is determined by the presence of elemental gold in the system. Normally it is a wall of a reaction vessel, a gold ampoule, which "…provided an abundant source of Au and buffered the Au activity close to one" (Fraley and Frank, 2014, p. 408). Hence, it is concluded that the determined values of the Au content in minerals within such a system (for example, sulfides) "…represent the solubility of gold in these sulfides at the experimental conditions and gold activity of 0.94 ± 0.01" (Jugo et al., 1999, p. 580). However, it is not clear how Au activity in an Au-based alloy or pure Au material relates to the state of the element in the sulfide. This choice of the standard state is incorrect, since Au is present in the structure of the sulfide not in the form of Au^o, as in an alloy or pure material, but in the ionic form (Au^+, Au^{3+}, possibly Au^-). Certainly, small quantity of the neutral Au atoms can also be present in the structure of a mineral, and for it such a choice of the standard state is formally acceptable. But in general, the Au content in the mineral will be determined by the activity of gold in the equilibrated with the mineral fluid, which may be different with different composition of the system (fluid, melt) in the same gold ampoule.

The above approach to the concept of solubility (S) of Au in a mineral usually leads to an underestimation of this value, unless the system achieves the activity of the dissolved Au forms that corresponds to saturation with respect to the phase of Au (real or virtual), which restricts its entry into the structure of the mineral. However, if the content of Au structural form is correctly determined, the result may be considered as a minimal value of solubility under the given test conditions ($S^{min}_{T,P,(a_{Au})\text{fl.}} \leq$ IL). By solubility, we mean Au incorporation limit (IL) into the structure regardless of its mechanism – isomorphic (IL = IC, that is, isomorphic capacity), or with the participation of defects in the crystal structure of the matrix – both intrinsic and extrinsic (Tauson, 1999a, 2005). In the case when defects are involved in the process of the admixture entrance, the concentration of the so-called defining or active defects (AD) becomes an essential parameter, in addition to the main T, P, $(a_{Au})_\text{fl.}$. They directly interact with the admixture atoms (ions), forming donor-acceptor pairs and more complex entities, and their concentrations in turn depends on intensive parameters, including not only $(a_{Au})_\text{fl.}$, but also, for example, aS_2, if these defects are the sulfur vacancies in the structure of the sulfide. IL can be defined as a constant only under maximum concentration of AD possible under given conditions, and IC, on the contrary, – in the absence of AD. This also applies to "extrinsic", i.e., admixture defects, which are often associated with a heterovalent Au isomorphism. Therefore, in order to compare and evaluate the reproducibility of experimental data, it is necessary to indicate for which phase (taken as the "standard" state) the saturation of the mineral with gold is considered, and what mechanism of incorporation and type of AD is assumed. This phase will be referred to as the reference phase, that is, the comparison phase. As

shown above, the metal Au cannot be such a phase. One of the goals of this work is to review the available experimental data taking into account the above features.

Another source of uncertainty with respect to Au IL is the method often used by experimenters for *in situ* deposition of mineral particles in the presence of dissolved Au, usually at low temperatures (≤ 200 °C). In the case of pyrite, small (~10–40 microns), inhomogeneous and highly defective precipitation particles are formed. It is not always clear how the authors manage to analyze the Au in them and correctly separate the volume and surficial components of the Au content (see below). In this case, the effect of duality of the distribution coefficient may appear, due to which the distribution coefficient of Au between the solid phase (pyrite, Py) and the solution aq ($D^{Py/aq}_{Au}$) remains relatively constant, but differs from the true one that corresponds to the structural form (Tauson et al., 2011). For pyrite precipitates obtained in the presence of As, ($D^{Py/aq}_{Au}$) varies from 50 to 1800 (Kusebauch et al., 2019). In the absence of As, it changes more than 2 times (Table S2 in the same work). Such variations indicate that the principle of "apparent" phase composition correlation is not fulfilled either (Urusov et al., 1997), and the system does not obey Henry's law even formally. The problem of size and perfection of crystals of the desired phase is also related to the need to separate Au^o form, that is, the elemental gold in the crystal unit or on the crystal surface in the form of micro- or nanoparticles. This problem is quite complex and is ignored in most works.

One of the possible options for absorbing an admixture of an incompatible element in the structural form is the mechanism of crystal growth through the medium of surficial nonautonomous phase (NAP), which can entail significant local enrichment of ore minerals with noble, rare earth metals and other trace elements (Tauson et al., 2018a,b, 2019a,b). This mechanism can either facilitate or hinder determination of Au solubility in minerals. The problem is complicated by the fact that the presence of SNAP requires a clear division of the element concentration into volume (structural) and surficial components. On the other hand, the property of NAP to act as a reference phase makes the task easier. The situation can be presented as follows (Tauson et al., 2019a). In the course of crystallization, it is the surface layer of the crystal and not the crystal core that is in equilibrium with the solution. Equilibrium is interpreted as equality of chemical potentials, taking into account the $\Delta\mu$ required for growth, that is, as a forced equilibrium under the influence of an extrinsic forcing factor (Tauson and Akimov, 1997). This layer is structurally reconstructed and chemically modified into NAP that is inseparable from the matrix crystal. The altered state of the layer is explained by the fact that the solid phase in equilibrium with an oversaturated solution is characterized by a higher value of the chemical potential compared to the solid phase in a saturated solution (Akhumov, 1987). An excess of μ can manifest itself both in the change of the structure of the surficial phase and in the change in its chemical composition (for example, the absorption of an admix-

ture incompatible with the bulk structure). As the thickness of the NAP layer increases, the moment comes when the layer sections adjacent to the matrix lose their diffusive connection with the oversaturated solution, and then part of the layer is transformed into a matrix crystal structure by the type of coherent or semi-coherent solid-phase transformation. In this case, the structure will include only as much of the element as it can accept according to the value of its solubility under these conditions. The element is found in NAP in a much higher concentration than in a matrix crystal and in a "suitable" chemical (ionized) form (at least partially). This allows us to consider NAP as a carrier of the properties of the reference phase (RP). The thickness of the NAP layer varies depending on the conditions and growth medium of the crystal, but does not exceed 1 μm. The contents of incompatible elements in the layer exceed their volume concentrations by thousands of times (gold in pyrite and magnetite, see (Tauson et al., 2011; 2012)). The problem is that SNAP, since it is in local equilibrium with the fluid, must also be maximally saturated with this element. For this purpose, it is proposed to use the so-called assisting elements (AE) that increase the content of the element in the fluid (Tauson et al., 1998; Tauson, 1999b). In the case of Au, As and Se were used: by varying the additives to the system of these elements, we obtained dependencies C_{Au}^{cr}–C_{AE}^{cr} between the content of structural admixture of Au in the crystal and the content of AE in it. The flat section of this curve, which corresponds to the saturation of the crystal with Au, was extrapolated to the zero AE content, thus obtaining Au IL in a "pure" mineral. This operation can be performed with a dependency C_{Au}^{cr}–C_{Au}^{fl}, but the determination of the Au content in the fluid requires the use of sampling techniques, which are not always reliable enough. The role of the reference phase can also be performed by an autonomous phase, which in this case is the so-called comparison mineral, CM (Tauson, 1999a,b), in which the forms and IL of the element under study in its structure are sufficiently well studied. Assuming that the system of co-existing (simultaneously growing) minerals obeys Henry's law and the principle of phase composition correlation, it is possible to estimate the IL of an admixture element in the studied mineral by extrapolating data on the interphase distribution to the impurity IL in the CM. We used greenockite (α-CdS) as a CM when studying the occurrence of Au in some concentrator minerals. In nature, greenockite does not pertain to main Au concentrators. Under relatively high sulfur fugacity, the AD for Au entry into greenockite are vacancies in the metal sublattice (Desnica-Frankovic et al., 1999), forming donor-acceptor pairs with interstitial gold atoms (v'_{Cd} – $Au^{\cdot}_i$). They are associated with the maximum gold IL, which is ~70 μg/g at $\lg f_{S_2}$ = –1.1 bar, 500 °C and a pressure of 1 kbar. At lower $\lg f_{S_2}$ ≤ –2.4 bar, it is 50 ± 10 μg/g at the same *P–T* parameters (Tauson et al., 2008). The minimum solubility of Au in CdS corresponds to a defect-free crystal and is associated with the traditional concept of isomorphic capacity, that is,

the miscibility limit of CdS and a hypothetical compound of AuS with the structure of α-CdS (wurtzite).

Given the above, it is necessary to consider experiments on the solubility (incorporation limit) of gold in minerals, taking into account a number of factors. These are the conditions of experiment, method of defining Au structural form (taking into account the size of the phase, important in the diagnosis and separation of Au modes of occurrence), type of the reference phase, and the mechanism of Au incorporation and the nature of active defects. In the absence of clarity regarding the reference phase, we will use the concept of minimum solubility estimation (S^{min} ≤ IL) formulated above. Data on the Au distribution coefficients between the mineral under study and the comparison minerals will also be involved, including extrapolation of the Au concentration to the IL in the CM, according to the phase composition correlation principle. The presentation of the entire set of available data on individual minerals is preceded by the original authors' developments that supplement and refine some of the previously obtained results.

EXPERIMENTS WITH Au-CONTAINING MINERAL ASSOCIATIONS

Problem statement. The need for additional experiments is due to the fact that individual IL estimates were obtained indirectly – through the coefficients of Au distribution between co-existing sulfides (Mironov et al., 1987, 1989; Tauson et al., 1996), by a qualitative method of comparing autoradiograms (Mironov et al., 1989, p. 141). Subsequently, the Au IL in some of them (galena, pyrrhotite) were refined (Tauson et al., 2008), but with the advent of the possibility of analysis by the LA-ICP-MS method, the accuracy of determining low Au contents increased, which made it necessary to repeat experiments on the synthesis of polyphase associations of this metal concentrator minerals.

Methods of experiment and analysis. The experiments were performed at 450 °C and a pressure of 1 kbar according to the standard method of thermogradient hydrothermal synthesis using internal sampling to determine the composition of a high-temperature fluid (Tauson et al., 2011, 2013, 2018a,b). Experiments were carried out in passivated titanium (VT-8) inserts for 24 days, and in the first 4 days the isothermal conditions were maintained for homogenization of the system, and in the next 20 days a temperature difference of 15 °C was created along the outer wall of the autoclave. The actual temperature gradient in titanium reaction containers did not exceed 0.1 deg/cm. The experiments were terminated by quenching the vessels in cold running water. Immediately after opening the inserts, the elements were completely removed from the trap by washing it with aqua regia and analyzed by atomic absorption spectrometry (AAS) on Perkin-Elmer M503, M403 (USA) devices. Diagnostics of the obtained phases was performed by X-ray phase analysis using an automatic D8 ADVANCE diffrac-

Table 1. Conditions and results of hydrothermal experiments on synthesis of multiphase associations and study of Au partitioning at 450 °C and 100 MPa

Exper. No.	Batch composition, wt.%*					Solution composition, wt.%	Solution in Sampler		Phases obtained**
	ZnS	PbS	Cu₂S	Fe	S		pH	Au, µg/g	
D28-1	30	30	20	20	–	5 NH₄Cl	7.9	1.0	Sph, Mt, Bn, Gn,Cpy
D28-2	30	30	20	20	–	10 NH₄Cl	7.5	0.62	Sph, Mt, Bn, Cpy, Gn
D28-3	30	30	20	20	–	10 NH₄Cl + 2 K₂Cr₂O₇	7.6	n.d.***	Sph, Mt, Gn
D28-4	30	30	10	15	15	5 NH₄Cl	6.5	1.94	Sph, Cpy, Py, Gn
D28-5	30	30	10	15	15	10 NH₄Cl	6.5	2.56	Sph, Py, Gn, Bn

*Weight of sulfide part of the charge is 6 g. Elemental Au is added as a foil (20 mg).
**Sph, sphalerite, Mt, magnetite, Bn, bornite, Gn, galena, Cpy, chalcopyrite, Py, pyrite.
***Not detected because of low volume of trapped fluid.

tometer (Brucker, Germany). Crystals in polymineral associations (Table 1) had sizes from fractions of a millimeter to 2–3 mm, the largest and most perfect of them were selected for analysis.

Particular attention was paid to the determination of Au, which was performed with two standard samples – laboratory sulfide standard MA4-1 (45 ± 3 ppm Au) and a standard sample of NIST 612 glass (4.9 ± 0.3 ppm Au). The measurements were performed on an Agilent 7500ce mass spectrometer with the New Wave Research UP-213 laser ablation platform (Agilent Tech., USA). The detection limit of Au amounted to 0.12 µg/g. Main parameters of analysis were as follows: plasma power 1400 W, flow rate of carrier gas 1.22 L/min, plasma-forming gas 15 L/min, laser power 90%, wavelength 213 nm, frequency 20 Hz, spot diameter 55 microns, number of channels per mass 3, scanning time of one channel 0.15 s, burn time 10 s. 3–4 points were taken in 5–6 crystals, and the contents of all the mineral-forming elements present in the system were monitored, which allowed us to filter out the cases of the point falling on the inclusion of another (co-existing) phase.

Results and discussion. Experimental conditions and phase analysis data are presented in Tables 1 and 2. Though Au contents in sphalerite are close to the detection limit, they positively correlate with the Au content in galena; the

principle of phase composition correlation is also fulfilled when the element is distributed between galena and bornite (Fig. 1). This indicates the structural nature of the Au admixture, which is most likely isomorphic, since it is difficult to expect the same behavior of the AD in such different structures. The situation is quite different in the experiments, where pyrite appears. There is a very high content of Au in galena (det. D28-4, Table 2), significantly exceeding its determined incorporation limit of 240 µg/g (Tauson et al., 2008). Thorough examination of the galena crystals obtained in this experiment reveals an interesting phenomenon. The crystals have a high blockiness, actually representing heteroepitaxial (syntactic) structures in which nanofilms of chalcopyrite and possibly other phases of copper are present on the cleavage faces of galena; they are perfectly visible even through a light microscope due to their characteristic reflectance. Apparently, these boundaries are highly active in the absorption of gold, similarly to the activity of dislocation pile-ups causing the effect of micro-admixture trapping (Urusov et al., 1997). In this case, we are most likely dealing with a phenomenon where the real crystal growth peculiarities have a critical influence on the absorption and distribution of admixture elements captured during crystallization. This entails absence of phase composition correlation between galena and pyrite, but in det. D28-5 we

Table 2. Results of Au LA-ICP-MS analysis in coexisting minerals synthesized in hydrothermal experiments at 450 °C and 1 kbar

Exper. No.	lgf_{S_2}, bar	Fe in Sph, wt.% (AAS)	Au ± σ, µg/g (LA-ICP -MS)[1]					
			Sph	Mt	Gn	Cpy	Bn	Py
D28-1	<–2.7[2]	2.8	0.16 ± 0.02	0.15 ± 0.02	73 ± 5	n.d.	42 ± 10	–
D28-2	<–2.7[2]	3.4	0.11 ± 0.02	≤0.1	28 ± 1	13 ± 5	17 ± 3	–
D28-3	–	4.1	0.14 ± 0.03	0.12 ± 0.02	47 ± 2	–	–	–
D28-4	–4.0[3]	1.8	≤0.1	–	(600 ± 30)[4]	15 ± 2	–	2 ± 2
D28-5	–3.7[3]	1.3	≤0.1	–	9.9 ± 0.3	–	10.2 ± 0.2	9.7 ± 0.2[5]

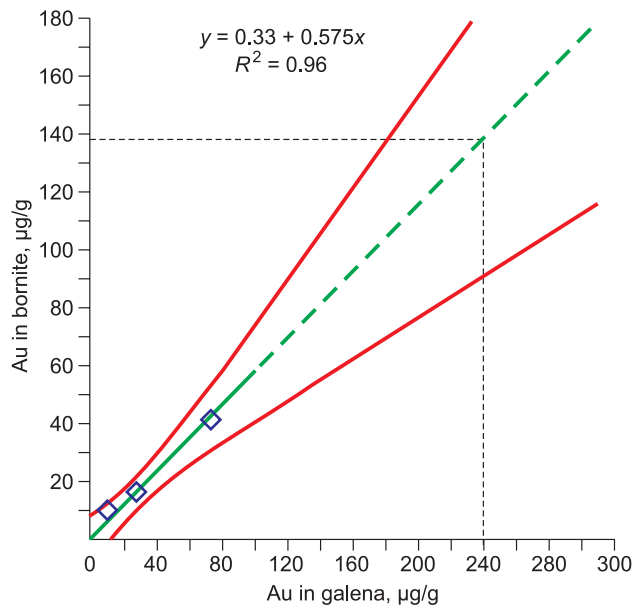Note. Dash indicates absence of phase in association.
[1]σ at confidence level of 95%.
[2]Estimated from equilibrium Cpy = Bn + Py.
[3]Estimated from sphalerite composition in the pyrite field.
[4]Explanation in text.
[5]Evenly distributed Cu in pyrite – 0.20 ± 0.07 wt.%.

$$y = 0.33 + 0.575x$$
$$R^2 = 0.96$$

Fig. 1. Diagram of phase composition correlation galena-bornite (Au distribution) based on the data of hydrothermal experiments. Au incorporation limit into bornite is estimated as ~140 μg/g.

Table 3. Gold solubility in minerals relative to galena as a comparison mineral according to the data of hydrothermal experiments at 450 °C, 1 kbar

Mineral	S_{Au}	$\bar{S}_{Au}$
Sphalerite	0.5 0.9 0.7	0.7 ± 0.3
Magnetite	0.5 0.6	0.6
Chalcopyrite	110	110
Bornite	138 146	140

experiment, we also assume the entry of Au with the formation of a neutral vacancy: $Au^+ + Cu^+ = Fe^{2+} + V_{Fe}$, especially since this mechanism seems to start acting at a slightly higher sulfur activity (Table 2). Using the previously specified incorporation limit of Au in galena, we shall perform the corresponding estimates of the solubility of the element in the remaining minerals of the obtained associations (Fig. 1; Table 3). The situation with pyrite will be discussed in detail below.

DATA ON THE SOLUBILITY OF GOLD IN MINERALS

Arsenopyrite. In the studies using the method of hydrothermal synthesis at temperatures of 400–500 °C and pressures of 1.5–2.0 kbar (Table 4), inhomogeneous in composition, zonal crystals of arsenopyrite were obtained. They were examined by the EPMA method. The paper (Wu and Delbove, 1989) presents averaged data for crystal zones, which are enriched with Au (1800–8000 μg/g) and depleted in it ($\leq$ MDL = 500 μg/g). The zones with high Au grade are characterized by a slightly higher As/S ratio compared to Au-poor zones (on average 1.16 and 1.11, respectively). A negative correlation of the atomic contents of Fe and Au

also observe another peculiarity – a fairly high Au content in pyrite at relatively low levels in co-existing galena and bornite. At the same time, Au is distributed very uniformly in all three minerals (the coefficient of variation is 2%!). In our view this is accounted for by the fact that pyrite in this experiment also has a uniform distribution of copper (0.20 ± 0.07 wt.%). If it forms a structural admixture in it, then the distribution of Au will depend on its content, and will not obey the Nernst's law in the same way (with the same distribution coefficient) as an ordinary isomorphic admixture. Au can enter pyrite by the mechanism of $Au^{3+} + Cu^+ = 2 Fe^{2+}$ (Chouinard et al., 2005), but due to a certain decrease in the parameter of the pyrite unit cell from this

Table 4. Data on Au solubility in arsenopyrite

No.	Experimental condition	Crystal size, μm	Au determination method[1]	Au solubility, μg/g[2]	Probable incorporation mechanism, active defect type	Ref.
1	Hydrotherm., 500 °C, 2 kb, Fe_2O_3–As–S–NaCl(HCl)-$AuCl_3$-H_2O	10–800	EPMA	17,000	Au↔Fe, As↔S?[3]	(Wu and Delbove, 1989)
2	Hydrotherm., 400–500 °C, 1.5 kb, FeS–As–NaCl–H_2O–Au (amp.)	≤10	EPMA	30,000	The same, +V_{Fe}	(Fleet and Mumin, 1997)
3	"Dry" system, 300–600 °C, 2–3 kb, natural material	Not specified	LA-ICP-MS	2.4–4.7	Not specified	(Tomkins and Mavrogenes, 2001)
4	Salt fluxes, 580–~520 °C, elements – Fe and S, sulfides, arsenides; Au – foil	≤5–200 (from photo)	LA-ICP-MS, XAS	23±14	Au↔Fe, Au°	(Trigub et al., 2017)
5	Salt fluxes, 450–~400 °C, 550–~500 °C, elements – Fe, As and S, sulfides, arsenides – FeS_2, FeAs; Au – wire	Up to 1000 (from photo)	EPMA	30,000	Au↔Fe	(Kovalchuk et al., 2019)

[1]EPMA, Electron Probe Microanalysis, LA-ICP-MS, Laser Ablation Inductively Coupled Plasma Mass Spectrometry, XAS, X-ray Absorption Spectroscopy.
[2]In absence of a definite referent phase the values are equal to $S^{min} \leq$ IL (see text for details).
[3]Negative correlation of Au and Fe in single crystal according to EPMA; As excess and S deficit in zones of elevated Au content.
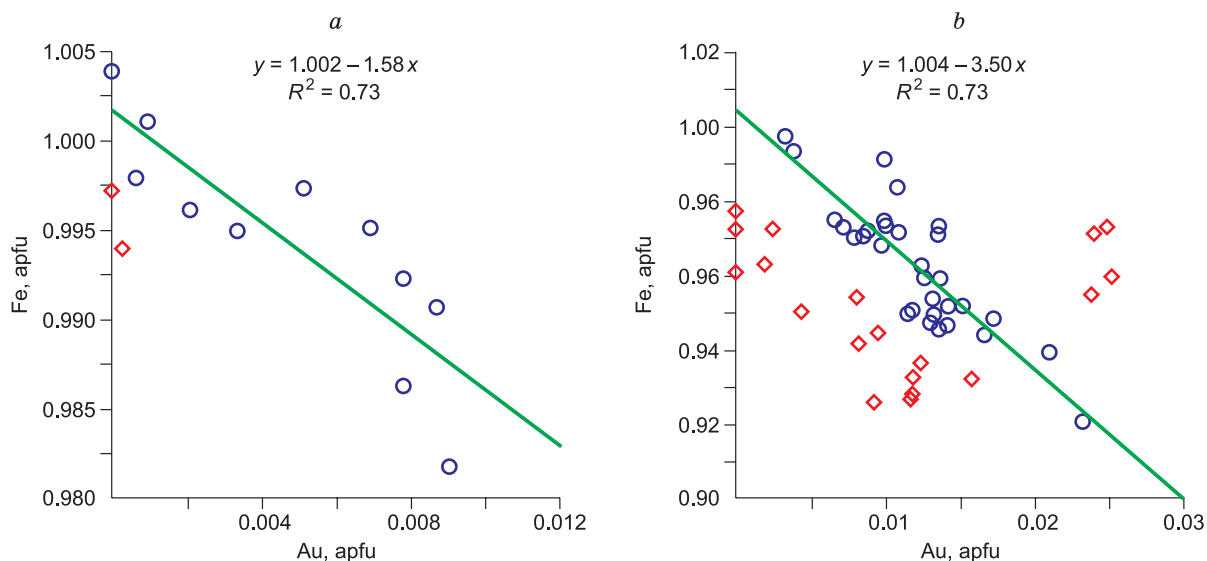
Fig. 2. Correlation between atomic quantities of Au and Fe in synthesized crystals of arsenopyrite according to Wu and Delbove (1989) (*a*) and Fleet and Mumin (1997) (*b*). Points shown as diamonds were not used in the approximating curve plotting because they appreciably reduced the coefficient of determination.

was observed within a single crystal (Fig. 2*a*), which allowed the authors to assume the substitution of Fe for Au in the structure of arsenopyrite. But it is possible that an increase in the As content also contributes to Au grade, although the Au-As correlation is less clearly expressed. Hydrothermal experiments similar in terms of conditions and results were later performed in the study (Fleet and Mumin, 1997) (Table 4). The Au content in arsenopyrite reached 3.0 wt.% (0.85 at.%) in the experiment at 400 °C, 1.5 kbar, 57 days. As in the previous work, the authors note the heterogeneity and chemical zoning of the crystals, despite their small size (about 10 microns). The composition of the main components is also variable: As varies from 27.2 to 41.5, S from 26.6 to 39.6 at.%. EPMA data on Au content in different growth zones of idiomorphic arsenopyrite grains revealed Fe deficiency and negative correlation of Au and Fe (Fig. 2*b*). This allowed the authors to assume the mechanism of gold entering the Fe position with a vacancy in the metal position – (Fe, Au, □) As$_{1\pm x}$S$_{1\pm x}$ (Fleet and Mumin, 1997). Most points with higher Au content correspond to As/S from 1.11 to 1.47, but there is no unambiguous correspondence: the same Au content may correspond to both of the above As/S values. In the works under consideration, the Fe–Au dependence is stronger than when replacing "atom by atom" (Fig. 2*a*, *b*), and assumes either the replacement of Fe with arsenic when Au is included, or the appearance of Fe vacancies.

Analyzing the materials considered, we tend to agree with the opinion (Wu and Delbove, 1989; Wu et al., 1990) about the existence of some special mechanism of crystallization of arsenopyrite under hydrothermal conditions, which leads to high concentrations of chemically bound (dissolved) gold in it, unusual needle morphology and distinct zoning of crystals, which the authors relate to a non-equilibrium

growth process. "Invisible" Au correlates with excess As in most natural and synthetic arsenopyrites (Fleet and Mumin, 1997). This is accounted for by the absorption of Au from the ore-forming fluid by chemisorption at surficial centers containing excess As and Fe deficiency, and the entry of Au into the composition of a metastable solid solution. But this model does not explain why this surface structure persists with continued growth, and how it enters the crystal volume, causing zoning in the distribution of As and Au. Chemosorption, which can only be responsible for the surface accumulation of the element, does not appear to explain this phenomenon, unlike the growth of arsenopyrite crystals by means of NAP, as a result of which the surface structure passes into the volume of the crystal (Tauson et al., 2019a).

Experimental modeling of the behavior of "invisible" gold in metamorphic reactions between arsenopyrite, pyrrhotite and löllingite showed that the increased content of the element is associated exclusively with the last of the listed minerals (407 ± 119 µg/g Au at 550–700 °C, 2–5 kbar). The transition of löllingite and pyrrhotite to arsenopyrite releases "invisible" gold from löllingite, but it is practically not included in arsenopyrite (2.4–4.7 µg/g, Table 4). The test with natural arsenopyrite containing "invisible" gold in the presence of H$_2$O in a gold ampoule at 600 °C and 3 kbar led to the exsolution of Au from it in the form of idiomorphic crystals. Although there is reason to doubt the achievement of equilibrium in these experiments observed by the authors (Tomkins and Mavrogenes, 2001), their results are of interest from the point of view of the possibility of using löllingite as a comparison mineral in the study of Au incorporation into arsenopyrite and pyrrhotite.

In recent years, studies have been performed on the synthesis of arsenopyrite and other sulfides in salt eutectic melts in the presence of Au (Trigub et al., 2017; Kovalchuk et al.,

2019). At the temperature of ~520 °C, it proved possible to saturate arsenopyrite with gold to ~23 µg/g (Table 4), and the authors concluded that the neutral form of Au replaced Fe. Kovalchuk et al. (2019) confirmed the relationship between Au and Fe and showed the possibility of not only Fe deficiency in arsenopyrite, as in the experiments (Fleet and Mumin, 1997), but also its excess (up to 2.1 at.%). For both compositions of arsenopyrite, enriched and poor in iron, negative correlations between Au and Fe are maintained, but their determination coefficients are low. However, these results confirm that formally one Fe atom is replaced by more than one Au atom. This may mean that part of the Au is embedded into the interstitials as $Au_i^\bullet$ or in the position of As^- as Au^-, and in case of iron deficiency, replacement of Au↔Fe is accompanied by the formation of a Fe vacancy or replacement of Fe with As.

According to the conditions of the experiments under consideration, a stationary temperature gradient of ~ 4.5 °C/cm was created in the ampoule (see Supplemental Materials to the article (Trigub et al., 2017)). The ampoule was placed horizontally in the furnace, which practically excluded convective temperature equalization, and in these conditions, the specified gradient is quite large. The temperature gradient can cause metastability and supersaturation of solid solutions. The appearance of inhomogeneous and zonal arsenopyrite crystals indicates significant instability of growth conditions. For example, in one of the samples, the Au content varied from < MDL to 1.42 wt.%, in the other – from <MDL to 3 wt.%. Variations in the composition of the main components are also significant (2–4 at.%).

In natural arsenopyrite, Au concentrations exceeding 1 wt.% (up to ~1.7 wt.%) (Cabri, 1992), are no exception. In pyrite at high concentrations of "invisible" form, Au is often present in two forms – chemically bound (structural) and elemental (native), represented by nano- or microparticles of free metal (Yang et al., 1998; Palenik et al., 2004), whereas in arsenopyrite, with rare exceptions (Genkin et al., 2002), the structural form prevails (Cabri et al., 1989). Its distribution is extremely heterogeneous. At the Le Chatelier deposit (France), electron-probe microanalysis of arsenopyrite reveals gold enrichment from the core to the periphery of the crystal from < MDL to 1.22 wt.% (Marcoux et al., 1989). This high heterogeneity and zoning of crystals is explained by the capture of Au during rapid non-equilibrium crystallization and changing parameters of T-P-f_{O_2} (Wu et al., 1990).

Pyrite. Studies on the synthesis of gold-containing pyrite and its concentration of dispersed Au have been carried out since the 1940s (Kuranti, 1941; Maslenitskii, 1944). Let's focus on the results obtained using quantitative methods and approaches (Table 5). These table data allow us to conclude that high values of Au solubility in pyrite, exceeding few parts per million, are observed only in the investigations without separation of the structural form of Au from the superficially bound one. This is especially true for experiments at low temperatures in the presence of As (Nos. 4 and 12 in

Table 5), in which fine particles of FeS_2 were formed, and total Au contents reached $(4–6)\cdot10^3$ µg/g. The results of growth experiments in which the size of crystals was at the level of millimeters, which allowed separating the volume and surface components of the Au concentration (Nos. 1, 5, 7, 8, and 13 in Table 5), differ sharply from the data obtained at low-dimensional, in fact, dispersed phases. The limit imposed by the presence of the reference phase – sulfide of Au and Ag (No. 9, Table 5): $C_{Au} < 240$ µg /g is extremely important.

Already the first experiments on the co-crystallization of pyrite and Au in the conditions of crystal growth have shown that evenly distributed Au is not present in the crystal body in any significant amount, but is located in a thin surface layer that "...does not exceed $n\cdot10^{-5}$ cm" (Mironov and Geletii, 1978), that is, several hundred nanometers. This result was subsequently confirmed by our growth experiments, which showed the presence on the surface of growing pyrite crystals of surficial non-autonomous phases of such thickness (~500 nm), capable of absorbing Au (as well as other trace elements) in concentrations by 3 orders of magnitude higher than in the volume of the crystal (Tauson et al., 2011, 2018a,b). Thus, the data of growth experiments leave no doubt that Au at the "hydrothermal" temperature and pressure parameters, over the entire stability interval of pyrite from its equilibrium with S^o to the border with pyrrhotite, is not incorporated into the structure of pyrite at concentrations above 1–3 µg/g. The limit of Au incorporation in pyrite may increase slightly (to about ~10 µg/g) when other admixture elements appear in its structure (Mn, Cu, Nos. 8 and 13 in Table 5; possibly As). Apparently, there is no phenomenon of Au retrograde solubility in pyrite (Deditius et al., 2014; Trigub et al., 2017); it is only a consequence of an incorrect interpretation of the results of experiments in which the separation of Au forms between the surface and the volume of crystals was not performed or was incorrectly performed due to the small size and low quality of the latter (defects, highly-developed internal surfaces). If we sum up the experimental and natural data on Au solubility in pyrite, we can obtain a concentration interval of at least 4 orders of magnitude. In most relatively high-temperature orogenic, magmatogenic-hydrothermal and hydrothermal-metamorphic deposits formed at temperatures from ~300 to 500 °C, the contents of "invisible" Au in pyrite are at the level of "equilibrium" concentrations of the structural form of gold established in our experiments (Tauson et al., 2019b). This is fully consistent with the values determined by the ADSSC method (analytical data selections for single crystals (Tauson et al., 2013)) for Au structural form in pyrite (≤5 µg/g, accuracy ±30 rel.%) at the deposits of different genetic types on the territory of the largest gold-bearing provinces of Russia and Uzbekistan (32 samples of pyrite from 11 deposits) (Tauson et al., 2014).

First-principle calculations, unfortunately, do not provide quantitative estimates for the occurrence of Au, although they confirm spectroscopic data on the charge state of gold

Table 5. Data on Au solubility in pyrite

No.	Experimental condition				Crystal size, μm	Au analysis method	Au solubility, μg/g[1]	RP or CM	Probable incorpor. mechanism, chem. form	Ref.
	T, °C	P, kb	$\lg f_{S_2}$, bar	Medium						
1	500	1	–	2M NH_4Cl	$(1–8)\cdot10^3$	ARG ^{195}Au	≤0.01	NAP?[2]	–	(Mironov and Geletii, 1978)
2	600	1.4	–2.2	1m KCl	$(3–5)\cdot10^2$	AAS	2 ± 0.43	–	–	(Cygan and Candela, 1995)
	700	1.4	–0.4	The same	The same	The same	6 ± 1^3	–	–	
3	450	1	≥–5.6	10% NH_4Cl, add. As, Se, Te	$n\cdot10^3$	EPMA, AAS	550 ± 300^3	NAP?	Au↔Fe, Au^{3+}	(Tauson and Smagunov, 1997)
4	405	1.5	–	KCl + H_2O, add. As	≤10	EPMA	3700^3	–	Au^o or Au^+	(Fleet and Mumin, 1997)
5	500	1	≤–2.4	10% NH_4Cl	$(1–5)\cdot10^3$	AAS-ADSSC, ARG ^{195}Au	3 ± 1	α-CdS	$Au'_{Fe} - v^{\cdot}_S(HS^{\cdot}_S)$	(Tauson, 1999b)
6	200	0.2	–	H_2S + NaOH + H_2O + Au (sol.)	1–2	AAS, XPS	3000^3	–	Au(I)	(Laptev and Rozov, 2006)
7	450	1	–	$NH_4Cl \pm Na_2S \pm$ HCl + H_2O	$(1–2)\cdot10^3$	AAS-ADSSC	1.2–3.6	NAP	–	(Tauson et al., 2011)
8	450	1	–5.6	10% NH_4Cl	≤10^3	AAS-ADSSC, XPS	$1–7.3^4$	NAP, α-CdS	$Au^+ + Mn^{3+} = 2Fe^{2+}$	(Tauson et al., 2013)
9	500	10^{-7}	–4.3	"Dry" system	<10	EPMA	$<240^3$	AgAuS	–	(Pal'yanova et al., 2015)
10	450	1	–1.4… –2.8	FeS + S + H_2O	<10	ICP-MS, XAS	86^3	–	Au↔Fe, Au^+	(Trigub et al., 2017)
11	450	0.7	–	0.5m $K_2S_2O_3$ + 0.3m KOH	<10–40	EPMA, RFA,XAS, LA-ICP-MS, SEM	204^3	–	S-Au-S	(Pokrovski et al., 2019)
	350	0.37	–	0.49m $K_2S_2O_3$ + 0.14m HCl			1664^3			
12	200	Sut. vap.	–16	$FeCO_3$ + 0.05m H_2S	10–40	LA-ICP-MS	1928 ± 777^3 5657^3 (with As)	–	Au^+	(Kusebauch et al., 2019)
13	450	1	–4.0	5% NH_4Cl	$n\cdot10^3$	LA-ICP-MS	2 ± 2	NAP, PbS	–	This work (Table 2)
			–3.7	10% NH_4Cl			9.7 ± 0.2^5		$Au^+ + Cu^+ = = Fe^{2+} + V_{Fe}$	

Note. ARG, Autoradiography; AAS, Atomic Absorption Spectrometry; EPMA, Electron Probe Microanalysis; ADSSC, Analytical Data Selections for Single Crystals (Tauson et al., 2013, 2018b), XPS, X-ray Photoelectron Spectroscopy, LA-ICP-MS, Laser Ablation Inductively Coupled Plasma Mass Spectrometry, XAS, X-ray Absorption Spectroscopy, XFA, X-ray Fluorescent Analysis, SEM, Scanning Electron Microscopy.

[1]In absence of a definite referent phase the values are equal to $S^{min} \leq$ IL.

[2]NAP, Nonautonomous Phase; question marks that NAP might be formed under the experimental conditions but was not studied.

[3]Bulk content: the separation of structural Au from the surficial form was not performed.

[4]Value 7.3 corresponds to pyrite enriched with Mn up to 0.3 wt.%.

[5]Pyrite contains evenly distributed (structural?) copper admixture (0.20 ± 0.07 wt.%).

Dash indicates the absence of data.

in pyrite to be Au^+ (Simon et al., 1999). The most likely models are the introduction of a gold atom into the interstitial position of the pyrite structure and its replacement of a sulfur atom (Chen et al., 2014). The latter does not seem strange due to the high probability of existence of anti-structural defects in pyrite with the formation energy of ~1.7 eV (Tomm et al., 1995).

There is no agreement on the mechanism of "excess" Au uptake by pyrite. It is believed that the entry of Au (I) into pyrite is controlled by the chemisorption of polysulfide complexes (-S-Au-S-(S-)$_n$). These complexes are "…partly incorporated in defects and dislocations by the growing pyrite crystal, and partly rejected from the structure by reduc-

tion to Au(0) during further pyrite life" (Pokrovski et al., 2019, p. 561). This model is unacceptable for the following reasons. First, pyrite demonstrates surface enrichment not only with gold, but also with other trace elements, both in experimental and in natural conditions (Tauson et al., 2018b, 2019b), which casts doubt on the hypothesis of a single complex responsible for the chemical state of Au. Second, high Au content in the surface is observed not only for pyrite and sulfides, but also for magnetite and hematite – oxides that crystallize in the absence of sulfur and, consequently, sulfide complexes (Tauson et al., 2012, 2016, 2018b). Third, the surface layers of crystals enriched with impurities behave thermodynamically as phases (NAP), and not as ad-

Table 6. Data on Au solubility in FeS – pyrrhotite (Po) and troilite (Tr)

No.	Phase	Experimental condition				Crystal size, μm	Au analysis method	Au solubility, μg/g[1]	RP or CM	Ref.
		T, °C	P, kb	lgf_{S_2}, bar	Medium					
1	Po	500	1	–4.3	2M NH$_4$Cl, add. Te, Se	$(5–8)\cdot 10^3$	ARG [195]Au	25 (add. Te)[3] 196(add. Se)[3]	NAP?[2]	(Mironov et al., 1989)
2	Po	600	1.4	–2.2	1m KCl	$(3–5)\cdot 10^2$	AAS	7 ± 1[3]	–	(Cygan and Candela, 1995)
		700	1.4	–0.4	The same	The same	The same	9 ± 2[3]	–	
3	Po	450	1	–5.6	10% NH$_4$Cl	$n\cdot 10^3$	EPMA	700	NAP?	(Tauson and Smagunov, 1997)
4	Po (Fe$_{0.81}$Cu$_{0.09}$)S	850	1	$–1 \pm 0.7$	0.15 M NaCl + 0.15 M KCl + 0.02 M HCl+0.02 M CuCl	–	EPMA	470 ± 100[3]	ISS	(Jugo et al., 1999)
5	Po (Tr) (Fe$_{1.0}$S)	450	1	–16.2	10% NH$_4$Cl, add. As, Se	$(1–2)\cdot 10^3$	AAS- ADSSC	25 ± 9	α-CdS	(Smagunov et al., 2004)
6	Po (Fe$_{0.87}$S)	450	1	–5.6	10% NH$_4$Cl, add. As, Se	$(2–3)\cdot 10^3$	The same	21	NAP	(Tauson et al., 2005)
7	Po	1050	10^{-2}	–1.3	"Dry" system with silicate and sulfide melts	<200	LA-ICP-MS	800[3]	–	(Simon et al., 2008)
8	Po (Fe$_{0.88}$S)	450	1	–5.6	10% NH$_4$Cl	$1.5\cdot 10^3$	AAS-ADSSC	4 ± 1	NAP, α-CdS	(Tauson et.al., 2013)
9	Po (Fe,Cu)S	800– 1000	2	–2…+0.2	H$_2$S + H$_2$O + silicate melt	–	LA-ICP-MS	$10–270$[3]	–	(Zajacz et al., 2013)
10	Po (Fe,Cu)S	600	1	$–2 \pm 1$	NaCl + KCl + HCl + H$_2$O	–	EPMA	500 ± 100[3]	ISS	(Fraley and Frank, 2014)
		700	1	–0.2… +0.4				$300–400$[3]		
11	Po	500	10^{-7}	–4.3	"Dry" system	<10	EPMA	<240[3]	AgAuS	(Pal'yanova et al., 2015)
	Tr	500	10^{-7}	–15				400 ± 130[3]	–	

Note. [1, 2, 3] see the notes in Table 5.
ISS, Intermediate Solid Solution Cu–Fe–S coexisting with Po and containing much more Au than pyrrhotite – probable reference phase although of variable composition.
 Dash indicates the absence of data.

sorbed complexes. The question of chemical and coordination state of Au in NAP is not finally resolved, as is the role of As in its concentration (Pokrovski et al., 2019). However, there is no doubt that the increased Au content (tens, hundreds, and even thousands of grams per ton, Table 5) is not related to the structural form of its presence in the volume of the pyrite crystal.

Pyrrhotite and troilite. The situation with iron monosulfide is as ambiguous as with iron disulfide (Table 6), although the variations in the estimation of the solubility of Au are much smaller and amount to a maximum of 2 orders of magnitude. Apparently, the cause for the discrepancies is different from that in the case of pyrite. The data is divided into two clusters – the first covers the Au content of 4–25 μg/g (Nos. 2, 5, 6 and 8), the second – 300–800 μg/g (Nos. 3, 4, 7, 10 and 11 Tr, Table 6); the intermediate position is occupied by Nos. 1 and 9. Belonging to one or another cluster does not seem to depend on the temperature and activity of sulfur in the system (and hence the composition of pyrrhotite). It is not yet clear with what this duality of Au behavior is related when it enters pyrrhotite. In the studies using EPMA, the heterogeneity of the composition in Au is often observed, and the element contents are close

to MDL, and acquisition of correct data requires serious statistical analysis. Concerning the question of the mechanism of Au occurrence in pyrrhotite, it is suggested that "…Au is contained in either vacancies or interstitial sites within the pyrrhotite lattice and is limited to 400 ± 100 μg/g" (Fraley and Frank, 2014, p. 416). However, the data presented in Table 6 shows that the entry of Au is not associated with Fe vacancies (compare Nos. 5, 6 and 11, Po and Tr). Perhaps due to the high degree of metallicity of the chemical bond in pyrrhotite, the entry of gold into its structure at the position of iron does not require the participation of defects and corresponding charge compensation, and in this case the Au IL in stoichiometric pyrrhotite becomes a "true" isomorphic capacity of FeS in Au (Tauson et al., 2008).

Chalcopyrite. Experimental data on Au solubility in chalcopyrite are limited. Several studies are devoted not to chalcopyrite itself, but to its "…high temperature equivalent, intermediate solid solution (Iss)", which "…may play an important role in sequestering gold from the melt" (Jugo et al., 1999, p. 574). The solubility of Au in ISS was estimated in the above work as 1.9 ± 0.4 wt.% at $T = 850$ °C and $P = 1$ kbar (see No. 4 in Table 6), the phase composition is Cu$_2$Fe$_3$S$_5$. In the field of "hydrothermal" parameters, the es-

timate by Mironov et al. (1987) of 250 µg/g at 500 °C, 1 kbar, which was later used to determine the solubility of Au in other sulfides (Tauson et al., 1996), was obtained by autoradiography of ^{195}Au. In the light of the results of this work (Tables 2 and 3), it seems to be overestimated. This is confirmed by the data of Simon's and co-authors' studies (Simon et al., 2000) conducted by the method of salt flux and solid-phase synthesis at 400, 500, 600, and 700 °C. At 500 °C, concentrations of Au in chalcopyrite from 5 to 16 µg/g were obtained, which is consistent with the data in Table 2. In the work mentioned above, ion-probe microanalysis was used to determine Au. It should be noted that there is no reason to consider the obtained values as the Au solubility, since there was no phase controlling saturation in the experiments, as there was no comparison mineral in them. As mentioned above, the presence of Au^o does not prove saturation of a sulfide solid solution with respect to chemically bound gold. At the same time, a very clear dependence of Au content on the temperature in the range of 400–600 °C was found, which may indicate the formation of a gold solid solution in CuFeS$_2$: 2–4 at 400, 5–16 at 500, and 100–125 µg/g Au at 600 °C. In this regard, the result of 110 µg/g obtained using galena as a reference mineral (Table 3), most likely corresponds to saturation at employed parameters (450 °C, 1 kbar).

High Au contents in ISS confirm the assumption (Mironov and Geletii, 1979; Jugo et al., 1999) that Au isomorphically replaces Cu in chalcopyrite. Indeed, the average length of the Fe–S and Cu–S valence bond (2.01 Å) almost coincides with this parameter for the Au-S (2.03 Å) bond (Brese and O'Keeffe, 1991). Theoretical analysis and simulation data of X-ray absorption spectra indicate a strong interaction between hybridized Au s,p,d, S p and Cu p,d orbitals, which causes the formation of gold-containing solid solutions in minerals of the Cu-Fe-S system (Tagirov et al., 2016). Apparently, for this reason, for chalcopyrite and ISS, there are no such discrepancies in the estimates of Au solubility, which we saw above for pyrite and pyrrhotite.

Bornite. The role of bornite as an Au concentrator is controversial. It is defined as an ineffective Au carrier (Cook et al., 2011), which fails to correlate with the ability of this mineral to absorb Au. Simon et al. (2000) in the experiments with salt melts showed that bornite contains an order of magnitude more Au than chalcopyrite (or ISS) at all the temperatures studied within the range of 400–700 °C. Au contents determined by ion-probe microanalysis are maximal in stoichiometric bornite and decrease both when the phase is enriched with copper and depleted in it. This seems to indicate that the occurrence of Au in bornite is not related to stoichiometric vacancies in its structure, but is isomorphic (Au$^+$↔Cu$^+$). At the same time, the regularity of increasing the Au content in stoichiometric bornite with a temperature of 13–80 at 400, 235–364 at 500, and 1280–8200 µg/g at 600 °C is clearly maintained. A lower estimate is given by Frank et al. (2011) for conditions of 800 °C, 1 kbar, in the medium of NaCl+KCl+HCl+H$_2$O; at lgf_{S_2} = –1.5 bar, the Au

content in bornite was 300 ± 80 µg/g. However, in a later work (Fraly and Frank, 2014) in the same system, but at lower sulfur fugacity, the maximum equilibrium concentrations of Au in bornite co-existing with ISS, according to EPMA data, amounted to 1000 ± 300, 1500 ± 300, and 1800 ± 300 µg/g at 500, 600, and 700 °C and lgf_{S_2} = –11, –8.3, and –6.0 bar, respectively. The authors observe that the solubility of Au in bornite increases with both temperature and f_{S_2}, but it is not possible to divide the contributions of each of these parameters into the solubility value. The result obtained in the present study is 140 µg/g at 450 °C using galena as a reference mineral and LA-ICP-MS for Au analysis (Fig. 1; Table 3) does not contradict the above data, taking into account their accuracy and variation intervals.

Galena. This mineral, as far as the authors know, has been scantily studied experimentally as a gold concentrator. But already in early works on hydrothermal synthesis of gold-containing ore sulfides, it was shown that, in contrast to pyrite and sphalerite, galena contains a uniformly distributed Au in the crystal body, possibly isomorphically replacing lead (Mironov and Geletii, 1979; Mironov et al., 1989). These works present the value of Au content equaling 73 µg/g for conditions of 500 °C, 1 kbar (synthesis in 2.06 M solution of ammonium chloride), and obtained using contrast autoradiography ^{195}Au. There is no evidence of reaching the incorporation limit because of lack of a limiting (reference) phase or a comparison mineral. In a later work (Tauson et al., 2008), the phase composition correlation principle was applied using a comparison mineral (greenockite) and AE (As and Se) at 500–520 °C, 1 kbar (synthesis in 10% NH$_4$Cl, sulfur fugacity at ~10^{-4} bar). The contents of the structural form were determined using atomic absorption spectrometry with electrothermal atomization and data processing using the method of ADSSC – analytical data selections for single crystals (Tauson et al., 2013). Au IL in galena amounted to 240 µg/g. The study of this system under different conditions (low f_{S_2}) and the analysis of the defective structure of PbS allowed us to assume that IL obtained in these experiments corresponds to the occurrence of gold in galena in the form of donor – acceptor pairs v$'_{Pb}$-Au$_i^{\bullet}$ (Tauson et al., 2008).

Sphalerite. The works cited above by Mironov et al. (1979, 1987, 1989) do not state the occurrence of Au in the structure of sphalerite at a concentration higher than the MDL of autoradiographic method, estimated by the authors as 0.01 µg/g. Results of the LA-ICP-MS analysis (Table 2) confirm the low, but still significant content of Au (0.11–0.16 µg/g) in sphalerite with low iron content (5–7 mol.% FeS). Using galena as a comparison mineral, we obtained Au IL in sphalerite of this composition of 0.7 ± 0.3 µg/g (Table 3). A similar value was obtained in the experiments on hydrothermal synthesis of ferrous sphalerite (22 mol.% FeS) at 500 °C, 1 kbar – 1 µg/g (Tauson et al., 1996). If the ratio of solubility S^{min}/S for more ferrous sphalerite remains the same as for a low-ferrous sphalerite, then the proportion can be used to estimate Au IL in ferrous

sphalerite as ~5 μg/g. The mechanism of incorporation (Tauson et al., 1996) involves participation of trivalent iron according to the scheme $Au^+ + Fe^{3+} \leftrightarrow 2\ Zn^{2+}$ (or $Zn^{2+} + Fe^{2+}$). The oxidation of Fe^{2+} to Fe^{3+} is accompanied by the formation of vacancies in the metal sublattice and becomes essential for the crystal chemistry of sphalerite at a FeS content above 12 mol.%. The proportion of Fe^{3+} increases with increasing f_{S_2} and amount, according to Mössbauer spectroscopy, 5–7% of total iron in a solid solution with 20 mol.% FeS at 700 °C (Lepetit et al., 2003). An increase in sulfur activity and an increase in Fe in sphalerite are antagonistic processes, so it is possible that the occurrence of Au in sphalerite with low iron content is partly due to the same donor-acceptor mechanism as for other mobile impurities in AIIBVI compounds – v'_{Me}–$Au_i^{\bullet}$.

Recently, studies have been conducted on the state of Au in In-sphalerite obtained at high temperature (850 °C) by a chemical transport reaction with a temperature gradient (Filimonova et al., 2019). EPMA, LA-ICP-MS, and X–ray absorption spectroscopy at the Au L_3 absorption edge were used. Au content reached 0.5 wt.%, gold was represented by the form Au^+ and was presumably incorporated into structure of solid solution $Zn_{1-2x}(Au,In)_xS$. It appears to have disintegrated as the system cooled, so that the predominant form of gold in sphalerite was Au_2S nanoclusters, although it is difficult to understand where such clusters can be found in the densely-packed (diamond-like) structure of sphalerite. However, these results allow us to explain the appearance of Au^o nanoparticles as a result of instability of gold sulfide formed during the transformation of the primary structural form (solid solution) of Au in the mineral during cooling or changes in redox conditions.

Magnetite. Like sphalerite, magnetite is a unique geochemical indicator. As a "transient" mineral, it also has wide isomorphic capabilities. Whether or not magnetite is one of Au concentrator minerals is still a subject of discussion (Mironov et al., 1989). We assume that, in contrast to pyrite, Au in magnetite is a compatible element (Tauson et al., 2012), so at low sulfur activity, the role of Au concentrator can shift from pyrite to magnetite (Smagunov and Tauson, 2003). An overview of Au solubility data in magnetite is presented in Table 7. By oxygen fugacity, most of the table data refers to conditions near the oxygen buffer NNO or MH. Under the conditions close to magnetite-hematite buffer, most experiments were performed with the control of the structural component of Au at 450 and 500 °C; since in a number of experiments, X-ray phase analysis diagnosed an admixture of hematite, the oxygen fugacity in them was at the level of $\lg f_{O_2} = -21.6$ and -19.2 bar, respectively (Tauson et al., 2016). Given the significant temperature range and differences in the chemical conditions of the experiments (in some cases, silicate melts were used), their results show good agreement, despite the fact that in some cases the data were obtained by the LA-ICP-MS method on microcrystals (Nos. 3 and 5, Table 7) with dimensions smaller than the diameter of the laser spot (Simon et al., 2003, 2008). The obvious exception is result No. 4, which is 2 orders of magnitude higher than the others. We see the explanation of this phenomenon in the fact that these experiments achieved high reduction conditions close to MI buffer in f_{O_2},

**Table 7.** Data on Au solubility in magnetite, Ti-magnetite and Mn-magnetite

No.	Phase	Experimental condition			Crystal size, μm	Au analysis method	Au solubility, μg/g[1]	RP or CM	Ref.
		T, °C	P, kb	Medium					
1	Mt	500	1	2.03 M NH₄Cl	$(0.4–2) \cdot 10^3$	AAS	2.5[3]	NAP?[2]	(Mironov et al., 1989)
2	Mt	600	1.4	1 m KCl	$(3–5) \cdot 10^2$	AAS	2 ± 0.4[3]	–	(Cygan and Candela, 1995)
		700	1.4	The same	The same	The same	3 ± 0.6[3]	–	
3	Mt	800	1.4	NaCl+KCl+ HCl+H₂O	4–12	LA-ICP -MS	2[3]	–	(Simon et al., 2003)
4	Mt	450	1	10% NH₄Cl	$n \cdot 10^3$	AAS- ADSSC	117 ± 55	Fe-greenockite	(Smagunov and Tauson, 2003)
5	Mt-Ulv	800	1	5% NaCl eq.	25	LA-ICP -MS	16 ± 9[3]	–	(Simon et al., 2008)
6	Mt	450	1	10% NH₄Cl ± HCl ± NaOH	$(0.5–3) \cdot 10^3$	AAS- ADSSC	0.5 ± 0.2	NAP	(Tauson et al., 2012)
7	Mt-Mn	450	1	10% NH₄Cl	$(1–2) \cdot 10^3$	AAS- ADSSC*	0.1–4.7	NAP, greenockite	(Tauson et al., 2013)
8	Mt	500	1	10% NH₄Cl	$(1–2) \cdot 10^3$	AAS- ADSSC, LA-ICP -MS	0.2	NAP	(Tauson et al., 2016)
8	Mt-Mn	500	1	10% NH₄Cl	$(0.5–1) \cdot 10^3$		1	–	
9	Mt	450	1	5% NH₄Cl, 10% NH₄Cl +2% K₂Cr₂O₇	$(0.5–1) \cdot 10^3$	LA-ICP -MS	0.6	NAP, galena	This work, Table 3

Note. [1,2,3] See the footnotes in Table 5.
*Several versions of ADSSC were used.
Note: Mt-Ulv, Ti-magnetite (magnetite-ulvöspinel series), Mt-Mn, Mn-magnetite (magnetite-jakobsite series).
Dash indicates the absence of data.
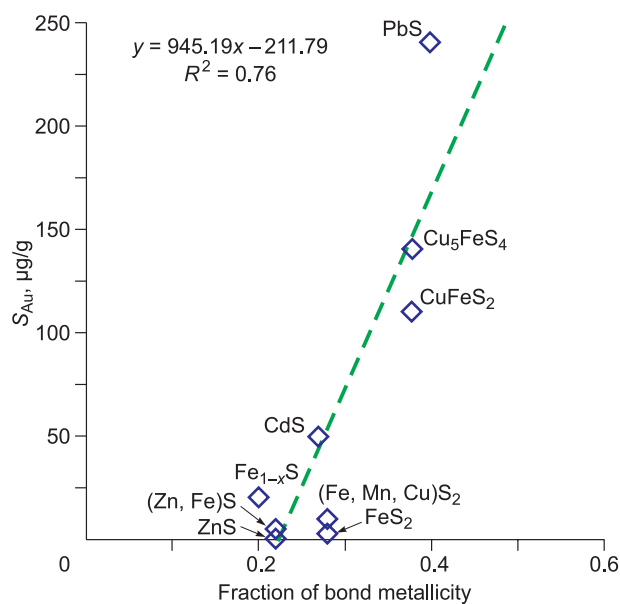
Fig. 3. Correlation of Au solubility and metallicity of chemical bond in sulfides – concentrators of noble metal.

and stoichiometric pyrrhotite $Fe_{1.0}S$ crystallized in association with magnetite (Smagunov and Tauson, 2003). This could lead to the formation of a uniformly distributed submicron-sized form of reduced gold Au^o in magnetite, which is indistinguishable from the structural form by the ADSSC method. Thus, the estimation of the Au IL in magnetite at 450–500 °C as ~1 µg/g seems optimal. With increasing temperature, IL changes insignificantly (Table 7).

Table 8 summarizes the most reliable, in our opinion, results on Au solubility, that is, data obtained with the separation of the structural form of Au in the presence of any limiting phase (autonomous or NAP), or by comparing with CM with a reliably established structural form of Au. In the vast majority, these are the results of hydrothermal experiments on the synthesis of mineral crystals at 450–500 °C,

Table 8. Au solubility in minerals in "hydrothermal" area of *P–T* parameters ($T = 450$–500 °C, $P \approx 1$ kbar)

Mineral	Formula	S_{Au}, µg/g
Sphalerite	ZnS	0.7
Fe-Sphalerite (marmatite)	(Zn,Fe)S	5
Magnetite	Fe_3O_4	1
Pyrite	FeS_2	3
Pyrite-Mn,Cu	$(Fe,Mn,Cu)S_2$	10
Pyrrhotite	$Fe_{1-x}S$	21
Chalcopyrite	$CuFeS_2$	110
Bornite	Cu_5FeS_4	140
Galena	PbS	240
Arsenpyrite	FeAsS	(30,000)*

*Probably metastable miscibility.

consistent (at least, not diverging within the order of magnitude) with the data of higher-temperature experiments. In accordance with the new data, the relationship between gold solubility and such a crystal-chemical parameter as the fraction of metallicity of the chemical bond in the mineral is clarified (Mironov et al., 1987). The metallicity of the bond (*m*) is characterized by a delocalized fraction of the covalent electron cloud; the criterion for absolute metallicity is the energy-gap width of the compound. We used the Batsanov equation (1989) for calculating *m*, the parameters of which were calculated earlier (Tauson et al., 1996). The results are shown in Fig. 3. They basically confirm the trend previously outlined (Tauson et al., 1996) of increasing Au solubility with increasing *m*, although, even with close metallicity of the bond, it is difficult to expect the same behavior of Au in non-isostructural compounds.

CONCLUSIONS

1. The solubility of gold in minerals is a multi-factor function and can only be correctly estimated if a number of conditions are met. Due to the influence of surficial nonautonomous phases on the element distribution, it is necessary to control the size and specific surface area of crystals in the experiments. The entry of Au into the structure through the use of "intrinsic" (own) and "extrinsic" (admixture) point defects makes it necessary to control the activity of sulfur and oxygen in the system and its composition in respect to admixture elements. The mechanism of crystal growth in experiments, in particular, growth by means of NAP, can definitely affect Au content causing imitation of high Au solubility in pyrite, arsenopyrite and galena (in nano-aggregates with copper sulfides). If it is taken into account, "false solubility" of Au observed in some experiments decreases by 1–3 orders of magnitude.

2. Sphalerite, magnetite and pyrite are characterized with low levels of S_{Au} (~1–3 µg/g), which are slightly increased when impurities enter the mineral structure (up to ~5 µg/g Au in Fe-sphalerite and ~10 µg/g in Mn- and Cu-containing pyrite and Ti-containing magnetite). Cu-containing sulfides (chalcopyrite, bornite), in which Au is most likely included as a true isomorphic admixture, possess lowest variability (S_{Au} = 110 and 140 µg/g, respectively, at 450–500 °C and 1 kbar). The dual situation with pyrrhotite (the availability of experimental data sets with Au content at the level of 4–25 and 300–800 µg/g) is not yet clear, but it is obviously not associated with Fe vacancies in its structure. At low activity of sulfur and oxygen, under reducing conditions, the formation of uniformly distributed submicroscopic form of Au^o in pyrrhotite and magnetite is possible, simulating the structural form and inseparable from it by analytical methods. Galena (S_{Au} =240 µg/g) is the most favorable sulfide matrix for locating Au atoms due to the high metallicity of chemical bond, which confirms the homogeneous distribu-

tion of the noble metal and a well-maintained phase composition correlation with greenockite and bornite, for which Au is a structural admixture.

3. The use of NAP as a reference phase in determining the limit of Au incorporation into minerals is theoretically and experimentally justified. The correlation between the solubility of Au and the degree of metallicity of the chemical bond in the mineral is defined more precisely; it has a sufficiently high coefficient of determination (0.76).

REFERENCES

Akhumov, E.I., 1987. Solid equilibrium phase with a supersaturated solution. Zhurnal Neorganicheskoi Khimii, No. 32 (1), 248–250.

Batsanov, S.S., 1989. Forbidden-band width and the coordination numbers of atoms. Izv. Akad. Nauk. Neorganicheskie Materialy, No. 25 (8), 1091–1095.

Brese, N.E., O'Keeffe, M., 1991. Bond-valence parameters for solids. Acta Cryst. B 47, 192–197.

Cabri, L.J., 1992. The distribution of trace precious metals in minerals and mineral products. Mineral. Mag. 56 (384), 289–308.

Cabri, L.J., Chryssoulis, S.L., De Villiers, J.P.R., Laflamme, J.Y.G., Buseck. P.R., 1989. The nature of "invisible" gold in arsenopyrite. Can. Mineral. 27 (3), 353–362.

Chen, J., Li, Y., Zhao, C., 2014. First principles study of the occurrence of gold in pyrite. Comput. Mater. Sci. 88, 1–6, doi: 10.1016/j.commatsci.2014.02.033.

Chouinard, A., Paquette, J., Williams-Jones, A.E., 2005. Crystallographic controls on trace-element incorporation in auriferous pyrite from the Pascua epithermal high-sulfidation deposit, Chile-Argentina. Can. Mineral. 43 (3), 951–963, doi: 10.2113/gscanmin.43.3.951.

Cook, N.J., Ciobanu, C.L., Danyushevsky, L.V., Gilbert, S., 2011. Minor and trace elements in bornite and associated Cu–(Fe)-sulfides: A LA-ICP-MS study. Geochim. Cosmochim. Acta 75, 6473–6496, doi: 10.1016/j.gca.2011.08.021.

Cygan, G.L., Candela P.A.,1995. Preliminary study of gold partitioning among pyrrhotite, pyrite, magnetite, and chalcopyrite in gold-saturated chloride solutions at 600 to 700 ºC, 140 MPa (1400 bars), in: Thompson, J.F.H. (Ed.), Magmas, Fluids, and Ore Deposits. Mineral. Assoc. of Canada Short Course 23 (6), pp. 129–138.

Deditius, A.P., Reich, M., Kesler, S.E., Utsunomiya, S., Chryssoulis, S.L., Walshe, J., Ewing, R.C., 2014. The coupled geochemistry of Au and As in pyrite from hydrothermal ore deposit. Geochim. Cosmochim. Acta 140, 644–670.

Desnica-Frankovic, I.D., Desnica, U.V., Stötzler, A., Deicher, M., 1999. Study of microscopic mechanisms of electrical compensation of donors in CdS by fast diffusors (Cu, Ag, or Au). Physica B 273–274, 887–890.

Filimonova, O.N., Trigub, A.L., Tonkacheev, D.E., Nickolsky, M.S., Kvashnina, K.O., Chareev, D.A., Chaplygin, I.V., Lafuerza, S., Tagirov B.R., 2019. Substitution mechanism in In, Au, and Cu-bearing sphalerites studied by X-ray absorption spectroscopy of synthetic and natural minerals. Mineral. Mag. 83 (3), 435–451, doi: 10.1180/mgm.2019.10.

Fleet, M.E., Mumin, A.H., 1997. Gold-bearing arsenian pyrite and marcasite and arsenopyrite from Carlin Trend gold deposits and laboratory synthesis. Amer. Miner. 82, 182–193.

Fraley, K.J., Frank, M.R., 2014. Gold solubilities in bornite, intermediate solid solution, and pyrrhotite at 500 to 700 ºC and 100 MPa. Econ. Geol. 109 (2), 407–418.

Frank, M.R., Simon, A.C., Pettke, T., Candela, P.A., Piccoli, P.M., 2011. Gold and copper partitioning in magmatic-hydrothermal systems at 800 ºC and 100 MPa. Geochim. Cosmochim. Acta 75, 2470–2482.

Genkin, A.D., Wagner, F.E., Krylova, T.L., Tsepin, A.I., 2002. Gold-bearing arsenopyrite and its formation conditions at the Olympiada and Veduga gold deposits (Yenisei Range, Siberia). Geol. Ore Depos. 44 (1), 52–68.

Jugo, P.J., Candela, P.A., Piccoli, P.M., 1999. Magmatic sulfides and Au: Cu ratios in porphyry deposits: an experimental study of copper and gold partitioning at 850 ºC, 100 MPa in a haplogranitic melt-pyrrhotite-intermediate solid solution-gold metal assemblage, at gas saturation. Lithos 46, 573–589, doi: 10.1016/S0024-4937(98)00083-8.

Kapitsa, S.P., 1991. Unscientific tendencies in the Soviet Union. In Science World, No. 10, 6–13.

Kovalchuk, E.V., Tagirov, B.R., Vikentyev, I.V., Chareev, D.A., Tyukova, E.E., Nikolsky, M.S., Borisovsky, S.E., Bortnikov, N.S., 2019. "Invisible" gold in synthetic and natural arsenopyrite crystals, Vorontsovka deposit, Northern Urals. Geol. Ore Depos. 61 (5), 447–468.

Kuranti, G., 1941. Synthetic study of gold-containing pyrite. Suiyokway-Si 10, 419–424.

Kusebauch, C., Gleeson, S.A., Oelze, M., 2019. Coupled partitioning of Au and As into pyrite controls formation of giant Au deposits. Sci. Adv. 5, eaav5891, doi: 10.1126/sciadv.aav5891.

Laptev, Yu.V., Rozov, K.B., 2006. Interaction of gold with sulfide surface as a factor of its concentration in hydrothermal ore formation. Dokl. Earth Sci. 411 (8), 1229–1232.

Lepetit, P., Bente, K., Doering, T., Luckhaus, S., 2003. Crystal chemistry of Fe-containing sphalerites. Phys. Chem. Minerals 30 (4), 185–191.

Marcoux, E., Bonnemaison, M., Braux, C., Johan, Z., 1989. Distribution de Au, Sb, As et Fe dans l'arsénopyrite aurifere du Châtelet de Villeranges (Creuse, Massif Central francais). C. R. Acad. Sci. Paris 308, 293–300.

Maslenitskii, I.N., 1944. On some cases of formation of dispersed gold segregations in iron sulfides. Dokl. Akad. Nauk SSSR 45 (9), 405–408.

Mironov, A.G., Geletii, V.F., 1978. Study of gold distribution in synthetic pyrites using Au-195 radioisotope. Dokl. Akad. Nauk SSSR 241 (6), 1428–1431.

Mironov, A.G., Geletii, V.F., 1979. Experimental investigation of gold distribution in sulfides. Dokl. Akad. Nauk SSSR 247 (1), 218–222.

Mironov, A.G., Tauson, V.L., Geletii, V.F., 1987. Metallicity of the bond as a factor controlling the inclusion of gold in sulfurous mineral structures. Dokl. Akad. Nauk SSSR 293 (2), 447–449.

Mironov, A.G., Al'mukhamedov, A.I., Geletii, V.F., Glyuk, D.S., Zhatnuev, N.S., Zhmodik, S.M., Konnikov, E.G., Medvedev, A.Ya., Plyusnin, A.M., 1989. Experimental Studies of Gold Geochemistry Using the Method of Radioisotope Indicators [in Russian]. Nauka, Novosibirsk.

Palenik, C.S., Utsunomiya, S., Reich, M., Kesler, S.E., Wang, L., Ewing, R.C., 2004. "Invisible" gold revealed: Direct imaging of gold nanoparticles in a Carlin-type deposit. Amer. Miner. 89, 1359–1366.

Pal'yanova, G., Mikhlin, Yu., Kokh, K., Karmanov, N., 2015. Experimental constraints on gold and silver solubility in iron sulfides. J. Alloys Comp. 649, 67–75.

Pokrovski, G.S., Kokh, M.A., Proux, O., Hazemann, J.-L., Bazarkina, E.F., Testemale, D., Escoda, C., Boiron, M.-C., Blanchard, M., Aigouy, T., Gouy, S., de Parseval, P., Thibaut, M., 2019. The nature and partitioning of invisible gold in the pyrite-fluid system. Ore Geol. Rev. 109, 545–563.

Simon, A.C., Pettke, T., Candela, P.A., Piccoli, P.M., Heinrich, C.A., 2003. Experimental determination of Au solubility in rhyolite melt and magnetite: Constraints on magmatic Au budgets. Amer. Miner. 88, 1644–1651.

Simon, A.C., Candela, P.A., Piccoli, P.M., Mengason, M., Englander, L., 2008. The effect of crystal-melt partitioning on the budgets of Cu, Au, and Ag. Amer. Miner. 93 (8–9), 1437–1448.

Simon, G., Kesler, S.E., Chryssoulis, S., 1999. Geochemistry and textures of gold-bearing arsenian pyrite, Twin Creeks, Nevada: Implications for deposition of gold in Carlin-type deposits. Econ. Geol. 94, 405–422.

Simon, G., Kesler, S.E., Essene, E.J., 2000. Gold in porphyry copper deposits: Experimental determination of the distribution of gold in the Cu-Fe-S system at 400 to 700 ºC. Econ. Geol. 95 (2), 259–270.

Smagunov, N.V., Tauson, V.L., 2003. Magnetite and pyrrhotite as potential gold concentrators at low sulfur activity. Dokl. Earth Sci. 392 (7), 995–998.

Smagunov, N.V., Tauson, V.L., Pastushkova, T.M., Nepomnyashchikh, K.V., 2004. Phase correspondence in gold distribution between concurrently growing greenockite and pyrrhotite crystals. Geochem. Int. 42 (11), 1062–1070.

Tagirov, B.R., Trigub, A.L., Kvashnina, K.O., Shiryaev, A.A., Chareev, D.A., Nickolsky, M.S., Abramova, V.D., Kovalchuk, E.V., 2016. Covellite CuS as a matrix for "invisible" gold: X-ray spectroscopic study of the chemical state of Cu and Au in synthetic minerals. Geochim. Cosmochim. Acta 191, 58–69.

Tauson, V.L., 1999a. Isomorphism and endocrypty: new approaches to study behavior of trace elements in mineral systems. Geologiya i Geofizika (Russian Geology and Geophysics) 40 (10), 1488–1494 (1468–1474).

Tauson, V.L., 1999b. Gold solubility in the common gold-bearing minerals: Experimental evaluation and application to pyrite. Eur. J. Mineral. 11 (6), 937–947.

Tauson, V.L., 2005. Systematics of processes of trace element uptake by real mineral crystals. Geochem. Int. 43 (2), 184–190.

Tauson, V.L., Akimov, V.V., 1997. Introduction to the theory of forced equilibria: General principles, basic concepts, and definitions. Geochim. Cosmochim. Acta 61 (23), 4935–4943.

Tauson, V.L., Smagunov, N.V., 1997. Effect of gold-accompanying elements on gold behavior in the Fe-S-aqua-salt solution system at 450 ºC and 100 MPa. Russian Geology and Geophysics (Geologiya i Geofizika) 38 (3), 667–674 (706–713).

Tauson, V.L., Lipko, S.V., 2015. Pyrite as a concentrator of gold in laboratory and natural systems: Structural incorporation and surface-related effect, in: Veress, B., Szigethy, J. (Eds.), Horizons in Earth Science Research. Nova Sci. Pub. Inc., New York, Vol. 12, pp. 87–120.

Tauson, V.L., Mironov, A.G., Smagunov, N.V., Bugaeva, N.G., Akimov, V.V., 1996. Gold in sulfides: state of the art occurrence and horizons of experimental studies. Russian Geology and Geophysics (Geologiya i Geofizika) 37 (3), 1–11 (3–14).

Tauson, V.L., Mironov, A.G., Bugaeva, N.G., Pastushkova, T.M., 1998. A method for estimating the ultimate concentration of gold inserted into mineral structures. Russian Geology and Geophysics (Geologiya i Geofizika) 39 (5), 628–633 (621–626).

Tauson, V.L., Smagunov, N.V., Pastushkova, T.M., 2005. Gold incorporation into pyrrhotite and the influence of nonautonomous phases on its distribution. Geochem. Int. 43 (1), 86–89.

Tauson, V.L., Smagunov, N.V., Akimov, V.V., Datkov, V.A., 2008. Mechanisms and species of gold incorporation into crystals of cadmium, lead, and iron sulfides. Russian Geology and Geophysics (Geologiya i Geofizika) 49 (8), 594–601 (784–793).

Tauson, V.L., Babkin, D.N., Pastushkova, T.M., Krasnoshchekova, T.S., Lustenberg, E.E., Belozerova, O.Yu., 2011. Dualistic distribution coefficients of elements in the system mineral-hydrothermal solution. I. Gold accumulation in pyrite. Geochem. Int. 49 (6), 568–577.

Tauson, V.L., Babkin, D.N., Pastushkova, T.M., Akimov, V.V., Krasnoshchekova, T.S., Lipko, S.V., Belozerova, O.Yu., 2012. Dualistic distribution coefficients of elements in the system mineral-hyd-

rothermal solution. II. Gold in magnetite. Geochem. Int. 50 (3), 227–245.

Tauson, V.L., Babkin, D.N., Akimov, V.V., Lipko, S.V., Smagunov, N.V., Parkhomenko, I.Yu., 2013. Trace elements as indicators of the physicochemical conditions of mineral formation in hydrothermal sulfide systems. Russian Geology and Geophysics (Geologiya i Geofizika) 54 (5), 526–543 (687–706).

Tauson, V.L., Kravtsova, R.G., Smagunov, N.V., Spiridonov, A.M., Grebenshchikova, V.I., Budyak, A.E., 2014. Structurally and superficially bound gold in pyrite from deposits of different genetic types. Russian Geology and Geophysics (Geologiya i Geofizika) 55 (2), 273–289 (350–369).

Tauson, V.L., Babkin, D.N., Pastushkova, T.M., Smagunov, N.V., Lipko, S.V., Voronova, I.Yu., Men'shikov, V.I., Bryanskii, N.V., Arsent'ev, K.Yu., 2016. Dualistic distribution coefficients of elements in the system mineral-hydrothermal solution. III. Precious metals (Au and Pd) in magnetite and manganmagnetite. Geochem. Int. 54 (2), 149–166.

Tauson, V.L., Lipko, S.V., Smagunov, N.V., Kravtsova, R.G., Arsent'ev, K.Yu., 2018a. Distribution and segregation of trace elements during the growth of ore mineral crystals in hydrothermal systems: geochemical and mineralogical implications. Russian Geology and Geophysics (Geologiya i Geofizika) 59 (12), 1718–1732 (2148–2165).

Tauson, V.L., Lipko, S.V., Smagunov, N.V., Kravtsova R.G., 2018b. Trace element partitioning dualism under mineral-fluid interaction: Origin and geochemical significance. Minerals 8 (7), 282.

Tauson, V.L., Lipko, S.V., Arsent'ev, K.Yu., Smagunov, N.V., 2019a. Crystal growth through the medium of nonautonomous phase: Implications for element partitioning in ore systems. Crystallogr. Rep. 64 (3), 496–507.

Tauson, V., Lipko, S., Kravtsova, R., Smagunov, N., Belozerova, O., Voronova, I., 2019b. Distribution of "invisible" noble metals between pyrite and arsenopyrite exemplified by minerals coexisting in orogenic Au deposits of North-Eastern Russia. Minerals 9 (11), 660.

Tomkins, A.G., Mavrogenes, J.A., 2001. Redistribution of gold within arsenopyrite and löllingite during pro- and retrograde metamorphism: Application to timing of mineralization. Econ. Geol. 96 (3), 525–534.

Tomm, Y., Schieck, R., Ellmer, K., Fiechter, S., 1995. Growth mechanism and electronic properties of doped pyrite (FeS₂) crystals. J. Cryst. Growth 146, 271–276.

Trigub, A.L., Tagirov, B.R., Kvashnina, K.O., Chareev, D.A., Nickolsky, M.S., Shiryaev, A.A., Baranova, N.N., Kovalchuk, E.V., Mokhov, A.V., 2017. X-ray spectroscopy study of the chemical state of "invisible" Au in synthetic minerals in the Fe-As-S system. Amer. Miner. 102, 1057–1065.

Urusov, V.S., Tauson, V.L., Akimov, V.V., 1997. Geochemistry of Solids [in Russian]. GEOS, Moscow.

Wu, X., Delbove, F., 1989. Hydrothermal synthesis of gold-bearing arsenopyrite. Econ. Geol. 84 (7), 2029–2032.

Wu, X., Delbove, F., Touray, J.C., 1990. Conditions of formation of gold-bearing arsenopyrite: a comparison of synthetic crystals with samples from Le Châtelet gold deposit, Creuse, France. Miner. Deposita 25, S8–S12, doi: 10.1007/BF00205244.

Yang, S., Blum, N., Rahders, E., Zhang, Z., 1998. The nature of invisible gold in sulfides from the Xiangxi Au-Sb-W ore deposit in northwestern Hunan, People's Republic of China. Can. Miner. 36, 1361–1372.

Zajacz, Z., Candela, P.A., Piccoli, P.M., Sanchez-Valle, C., Wälle, M., 2013. Solubility and partitioning behaviour of Au, Cu, Ag and reduced S in magmas. Geochim. Cosmochim. Acta 112, 288–304, doi: 10.1016/j.gca.2013.02.026.

Editorial responsibility: V.S. Shatsky